Dynamic polarizability of an atomic ion within a dense plasma

Joyee Basu* and Debasis Ray†

Department of Physics, Bengal Engineering & Science University, Shibpur, Howrah 711 103, West Bengal, India

(Received 22 September 2010; published 31 January 2011)

We analyze the influence of plasma electron density on frequency-dependent linear field-response behavior of an atomic ion embedded in a dense plasma medium. The frequency-dependent atomic response, characterized by the dynamic dipole polarizability $\alpha_d(\omega)$ as a function of the angular frequency ω of the time-dependent field, is estimated here up to the first pole of $\alpha_d(\omega)$ on the ω axis (corresponding to the lowest resonance transition $1s^2\,{}^1S \rightarrow 1s2p\,{}^1P$) for the ground state $1s^2\,{}^1S$ of a two-electron atomic ion Ne^{8+} ($Z=10$) at different plasma electron densities, as a typical example, employing the time-dependent coupled Hartree-Fock scheme within the framework of the ion-sphere model. It is observed that, owing to plasma density-induced enhancement of $\alpha_d(\omega)$ at every ω, the pole position of $\alpha_d(\omega)$ on the ω axis retracts toward the origin. This indicates a density-induced lowering (redshift) of the corresponding transition energy that conforms to experimentally observed trends. The polarizability calculation suggests a density-induced drop in the $1s^2\,{}^1S \rightarrow 1s2p\,{}^1P$ absorption oscillator strength in the atomic ion within dense plasmas.

DOI: 10.1103/PhysRevE.83.016407 PACS number(s): 52.25.Os, 32.10.Dk, 52.25.Vy, 31.15.ag

I. INTRODUCTION

The past three decades have witnessed remarkable progress in the theoretical simulation of plasma screening effects on electronic structures, properties, and processes of atomic ions immersed in a variety of plasma environments. The most striking spectroscopic signatures of a dense plasma medium on electronic properties of a plasma-embedded atomic system are enshrined in the phenomena of continuum lowering and the plasma polarization redshift [1] of atomic transition energy that have received serious attention and have undergone rigorous scrutiny by experimentalists and theoreticians alike. Accurate experiments spanning over the years have confirmed the lowering of atomic ionization continua and atomic line broadening as well as redshifts of the center of gravity of the lines in the presence of dense laser-produced plasmas. These phenomena may be ascribed primarily to the modification of electronic structures of atoms induced by the screening effects of perturbing plasma charges surrounding them. The theory of atomic line shifts in plasmas has been developed employing a variety of theoretical techniques [1], and the diagnostic potential of the phenomenon was also pointed out [2]. The theoretical efforts to extract plasma-induced atomic line shifts have relied essentially upon the traditional time-honored route for deriving the transition energy from the differences in computed energy levels of plasma-perturbed atomic systems, and the results clearly indicate energy shifts toward the red end of the spectrum. In particular, a detailed computation incorporating the contributions of the $\Delta n = 0$ transitions to the linewidths and shifts of H and He^+ in the dipole approximation produced results that are in good agreement with experiment [1]. In recent years, several other aspects of atomic structures and properties in various plasma backgrounds have received the growing attention of the theoreticians. These include electric multipole oscillator strengths [3] and magnetic multipole transition rates [4] in a stripped heliumlike ion, hydrogenic fine structures [5] and the diamagnetic response of a two-electron atomic ion [6,7], photoionization of hydrogenlike ions [8] and alkali atoms [9], doubly excited autoionizing states of the H^- ion, the Ps^- ion, and neutral helium [10–12], positron annihilation in the Ps^- ion [13], Stark shifts and widths of a hydrogen atom [14] and static dipole polarizabilities of hydrogenlike ions [15], relativistic effects in the spectra of hydrogenlike ions [16], the dipole oscillator strengths for low-lying transitions in helium and lithium atoms [17], and the lowest allowed and intercombination transitions in berylliumlike ions [18,19]. Very recently, the plasma effects on stability, bound states, and dipole polarizability of a hydrogen molecular ion H_2^+ have been addressed theoretically [20,21]. Of late, the dynamics of $He^{2+} + H(1s)$ excitation and electron capture processes [22] and of the photoionization of hydrogenlike ions [23], as well as atomic multiphoton transitions [24–27] in plasma environments, also have been the subjects of theoretical investigation.

It appears that the influence of a plasma medium on frequency-dependent field-response behavior of plasma-embedded atomic systems has received little attention to date. In this paper we explore the plasma-induced modification in the linear response of the bound electrons of a plasma-embedded atomic ion to an external monochromatic radiation field of angular frequency ω. The frequency-dependent (or dynamic) polarizability $\alpha(\omega)$, which is the Fourier transform of the time-dependent response function, is the key quantity in the present study. It is a well-known fact that $\alpha(\omega)$ explodes whenever the incident frequency ω coincides with any of the atomic transition frequencies, and thus it is possible to extract the atomic transition frequencies from a study of the "poles", i.e., the divergences of $\alpha(\omega)$ on the ω axis. Hence, an interpretation of plasma-induced modification in atomic transition frequency should be possible in the light of plasma-modified $\alpha(\omega)$ and its modified pole positions, and this new possibility provides us the motivation for the present study. In other words, the frequency-dependent behavior of $\alpha(\omega)$ in dense plasmas should bear the evidence of a plasma polarization redshift, and thus the present approach might offer

*joyeebasu@yahoo.com
†ray.debasis@gmail.com

an alternative and hitherto much less explored route for probing atomic line shifts in plasmas. The theoretical steps involved in our study are presented in Sec. II of this paper. The results and discussion are then given in Sec. III, followed by the conclusion in Sec. IV.

II. THEORETICAL METHOD

In this calculation we typically exemplify the case of a heliumlike two-electron atomic ion Ne^{8+} ($Z = 10$) in dense plasmas, characterized by the unperturbed (field-free) Hamiltonian

$$H_0 = \sum_{j=1,2}\left[-\left(\frac{\hbar^2}{2m}\right)\nabla_j^2 - \left(\frac{Ze^2}{r_j}\right) + V_{pj}\right] + \frac{e^2}{r_{12}}. \quad (1)$$

V_{pj} is the additional potential energy felt by the bound atomic jth electron owing to the presence of the surrounding plasma medium. For the sake of numerical convenience, in our calculation V_{pj} is constructed using the uniform-density ion-sphere (or Wigner-Seitz sphere) model [28,29]. This model is a relatively simple yet reasonable approximation for describing the effects of density-induced static plasma screening on atomic properties, and is suitable when the plasma is mildly strongly coupled. The model is known to make qualitatively correct predictions of plasma density effects on atomic structures, and therefore has been used earlier to investigate atomic phenomena in such plasmas [5,7,30,31].

In the uniform-density ion-sphere model, the test atomic ion in question, with a nuclear charge $+Ze$ and n_b (=2) number of bound electrons, is posited at the center of a sphere of radius R_0 containing a homogeneous distribution of n_f ($=Z-n_b$) number of plasma electrons that neutralize the net charge of the ion, with n_e being the local density of free plasma electrons. The ion-sphere radius R_0 is expressed as

$$R_0 = \left(\frac{3n_f}{4\pi n_e}\right)^{1/3}. \quad (2)$$

It is evident from Eq. (2) that at higher plasma electron densities, the charge neutralization of the test atomic ion occurs within ion spheres of smaller radii. The electrostatic potential energy seen by the bound atomic electron at r_j owing to the presence of plasma electrons within the ion sphere (only the static screening is considered in this model) is then given by

$$V(r_j; R_0) = \left(\frac{e^2 n_f}{2R_0}\right)\left[3 - \left(\frac{r_j}{R_0}\right)^2\right] \equiv V_{pj} \quad (r_j < R_0). \quad (3)$$

The total potential and its first derivative vanish at the ion-sphere boundary. Beyond the ion-sphere boundary, the positive charge distribution is assumed to neutralize exactly the negative electron distribution, thereby producing an electrically neutral background.

The atomic ion is in the spherically symmetric (with no permanent electric dipole moment) plasma-modified ground state $1s^2\,{}^1S$ with energy E_0 and a normalized wave function $\Psi_0(\mathbf{r},t) = \Psi_0(\mathbf{r})\exp(-iE_0t/\hbar)$. E_0 and $\Psi_0(\mathbf{r})$ are obtained with sufficient accuracy from a variational Hartree-Fock-Roothaan (HFR) solution to the unperturbed Hamiltonian of Eq. (1) by the basis set expansion technique [32,33], corresponding to different values of the ion sphere radius R_0 (or, equivalently, at different plasma electron densities n_e). In what follows, we have adopted (unless stated otherwise) atomic units (a.u.) in which $e = m = \hbar = 1$, the unit of length $= a_B = \hbar^2/me^2 = 0.529\,177$ Å, and the unit of energy$= 2$ Ry $= |-me^4/\hbar^2| = 27.2116$ eV. The probe electromagnetic field imposed on the plasma-embedded atomic system is modeled in the field gauge [34] as a dipolar harmonic perturbation of the form

$$H' = \sum_{j=1,2}[h(\vec{r_j})e^{-i\omega t} + \text{c.c.}], \quad (4)$$

where $h(\vec{r}) \sim r\cos\theta$ and c.c. denotes the complex conjugate. For the sake of numerical convenience, it is assumed that the applied field is weak enough so that the uniform plasma electron distribution within the ion sphere is left undisturbed, and the resulting potential V_{pj} remains spherically symmetric. Now, the dynamic response of the bound-electron cloud in the ground state of the atomic ion under the influence of this time-dependent dipolar driving field may be expressed in terms of the frequency-dependent or dynamic dipole polarizability (of the ground state) as [34]

$$\alpha_d(\omega) = \sum_{n\neq 0}\left|\langle\Psi_0|\sum_{j=1,2} z_j|\Psi_n\rangle\right|^2 \times\left(\frac{1}{E_n - E_0 + \omega} + \frac{1}{E_n - E_0 - \omega}\right). \quad (5)$$

Ψ_n is the nth excited wave function of the unperturbed two-electron Hamiltonian H_0, with a corresponding energy E_n. The estimation of $\alpha_d(\omega)$ using this formula entails the job of evaluating the infinite sum in Eq. (5) over the excited states including the continuum. This is accomplished in the present calculation via a time-dependent variation-perturbation procedure [35–38] within the framework of the coupled Hartree-Fock approximation, which allows us to write $\alpha_d(\omega)$ in terms of the unperturbed and the first-order perturbed one-electron orbitals in the following way:

$$\alpha_d(\omega) = \sum_k[\langle\delta\psi_k^-|r\,\cos\,\theta|\psi_k\rangle + \langle\delta\psi_k^+|r\,\cos\,\theta|\psi_k\rangle]. \quad (6)$$

The unperturbed ground-state orbitals ψ_k are already known from the HFR solutions to H_0 and have been used to construct Ψ_0. The first-order perturbed admixtures $\delta\psi_k^{\pm}$ to ψ_k, induced by the two components of the perturbing field, are to be determined variationally via the following steps. First, we introduce the time-dependent, normalized variational functional [39–41] of the Dirac-Frenkel type, averaged over the complete cycle of the applied field,

$$J[\Phi] = \left(\frac{1}{T}\right)\int_0^T dt\,\frac{\langle\Phi|H - i\frac{\partial}{\partial t}|\Phi\rangle}{\langle\Phi|\Phi\rangle}, \quad (7)$$

and subject to the optimization condition,

$$\delta J[\Phi] = 0. \quad (8)$$

Φ stands for the field-perturbed ground-state wave function corresponding to the total perturbed Hamiltonian $H = H_0 + H'$ in the presence of the external field, and may be expressed

by means of the normalized antisymmetrizer $\boldsymbol{A}$ in the following manner [35–38] (through first-order):

$$\Phi(\vec{r},t) = e^{-iE_0t}\boldsymbol{A}\prod_k(\psi_k + \delta\psi_k^- e^{-i\omega t} + \delta\psi_k^+ e^{i\omega t}). \quad (9)$$

The radial parts of the first-order perturbed orbitals are represented by a linear combination of suitable Slater-type bases of dimension p (i.e., the number of parameters, which is usually $\leqslant 12$) and with preassigned exponents $\{n_{kp},\rho_{kp}\}$:

$$\delta\psi_k^{\pm}(r) = \sum_p C_{kp}^{\pm} r^{n_{kp}} e^{-\rho_{kp}r}. \quad (10)$$

The unknown coefficients of expansion, $C_{kp}^{\pm}$, are then obtained through a linear variation procedure following the variational condition $(\partial J/\partial C^{\pm}) = 0$, which leads to a set of linear inhomogeneous equations to be solved. This completes the knowledge of the first-order functions, which are then utilized to estimate $\alpha_d(\omega)$ from Eq. (6).

The presence of a resonant denominator in the expression for $\alpha_d(\omega)$ in Eq. (5) indicates that $\alpha_d(\omega)$ diverges as the external field frequency ω approaches the excitation energy $\omega_{n0} = E_n - E_0$ for the nth excited state, and has a singularity (or pole) at $\omega = \omega_{n0}$. The dipolar driving field of the angular part $\sim Y_{10}$ acting on the ground state 1^1S of angular character Y_{00} results in excited states of Y_{10} symmetry, i.e., only those excited states $1snp\,^1P$ that are dipole connected to the ground state $1s^2\,^1S$ contribute in the present case in Ψ_n within the summation with their respective energies E_n, and the first pole to be encountered on the real ω axis is the one corresponding to the $1s2p\,^1P$ state. Reverting to the orbital representation of α_d in Eq. (6), its dependence on ω is implicit, coming through the ω dependence of $C^{\pm}$ in $\delta\psi_k^{\pm}$ as obtained from the solution of the variational equations. As the external input ω tends to the transition frequency $\omega(1s^2\,^1S \rightarrow 1s2p\,^1P)$ at the first pole of $\alpha_d(\omega)$, the radial part of the first-order perturbed orbital $\delta\psi_{1s}$ (of angular character Y_{10}) there assumes the $2p$-orbital character, after renormalization of the divergent function. Therefore, by adjusting ω to match the resonance condition, the energy (or the line frequency) for the $1s^2\,^1S \rightarrow 1s2p\,^1P$ transition in the atomic ion can be extracted. This is done here by increasing ω in suitable steps starting with zero and up to a chosen neighborhood of the first resonance, and thereafter performing finer scanning in the close vicinity of the resonance with a much reduced step size in order to pinpoint the pole with a desired level of accuracy.

III. RESULTS AND DISCUSSION

The results are presented in Table I, where $\alpha_d(\omega)$ as a function of ω is tabulated for the isolated (i.e., $n_e = 0$) atomic ion, and for the ion immersed in dense plasmas characterized by four different electron densities. Referring to the column corresponding to n_e=0, it can be seen that, initially, $\alpha_d(\omega)$ increases monotonically with ω at a slow pace. This is followed by a gradually steeper rise on approaching the resonance, which finally culminates in a "blowup" at the pole ($\omega = 33.8718$ a.u.). The pole position compares well with the transition energy 33.8836 a.u. of Vainshtein and Safronova [42] for the $1s^2\,^1S \rightarrow 1s2p\,^1P$ transition, and also the magnitude 0.001 044 a.u. of the static dipole polarizability α_d ($\omega = 0$) agrees with the value 0.001 045 a.u. quoted by

TABLE I. Frequency-dependent dipole polarizability $\alpha_d(\omega)$ (in a.u.) of the ground state $1s^2\,^1S$ of a Ne^{8+} atomic ion as a function of the field frequency ω (in a.u.), at different plasma electron densities n_e (in 10^{24} cm^{-3}).

	$\alpha_d(\omega)$				
ω	$n_e = 0$	$n_e = 1.611$	$n_e = 5.867$	$n_e = 9.684$	$n_e = 12.89$
0.0	1.044 (−3)[a]	1.045 (−3)	1.050 (−3)	1.055 (−3)	1.058 (−3)
10.0	1.123 (−3)	1.125 (−3)	1.131 (−3)	1.137 (−3)	1.142 (−3)
20.0	1.474 (−3)	1.480 (−3)	1.495 (−3)	1.509 (−3)	1.521 (−3)
30.0	3.65 (−3)	3.74 (−3)	4.01 (−3)	4.35 (−3)	4.77 (−3)
31.0	4.66 (−3)	4.82 (−3)	5.42 (−3)	6.33 (−3)	7.94 (−3)
31.5	5.46 (−3)	5.72 (−3)	6.73 (−3)	8.62 (−3)	1.47 (−2)
31.8	6.13 (−3)	6.49 (−3)	7.96 (−3)	1.14 (−2)	1.12 (−1)
31.8245					7.00 (+1)
32.0	6.69 (−3)	7.14 (−3)	9.12 (−3)	1.49 (−2)	
32.3	7.80 (−3)	8.47 (−3)	1.19 (−2)	3.18 (−2)	
32.5	8.80 (−3)	9.72 (−3)	1.51 (−2)	3.28 (−1)	
32.5192				1.90 (+2)	
32.8	1.10 (−2)	1.26 (−2)	2.68 (−2)		
33.1	1.49 (−2)	1.84 (−2)	1.78 (−1)		
33.1496			1.02 (+2)		
33.4	2.37 (−2)	3.60 (−2)			
33.6	4.03 (−2)	1.09 (−1)			
33.6948		1.23 (+2)			
33.7	6.31 (−2)				
33.8	1.49 (−1)				
33.8718	2.09 (+2)				

[a] $M(\pm N) \equiv M\times 10^{\pm N}$.

Thornbury and Hibbert [43]. A similar ω-dependent behavior of $\alpha_d(\omega)$ is noticed also at nonzero plasma electron densities. However, from the tabulated set of data, the following features are evident: (i) At $\omega = 0$, the static polarizability $\alpha_d(0)$ of the bound-electron cloud is larger at higher plasma electron densities, and the same is also true for the dynamic polarizability $\alpha_d(\omega)$ at any $\omega \neq 0$, and (ii) at a frequency ω, the rate of change of $\alpha_d(\omega)$ with ω increases as n_e becomes larger. Consequently, the $\alpha_d(\omega)$ curve at a higher density rises faster and reaches infinity at a frequency lower than that for a curve at a lower density. In other words, for higher densities, the resonance condition is satisfied at increasingly lower frequencies and the pole positions are retracted toward the origin. This means, the line frequency corresponding to the atomic transition $1s^2\,{}^1S \rightarrow 1s2p\,{}^1P$ is reduced, i.e., redshifted. The physically interesting portions of the contents of Table I are delineated graphically in Fig. 1, where the polarizability graphs at the four nonzero densities in increasing order are represented by B, C, D, and E, with their respective pole positions ω_B (=33.6948 a.u.), ω_C (=33.1496 a.u.), ω_D (=32.5192 a.u.), and ω_E (=31.8245 a.u.) marked and compared against the free-ion ($n_e = 0$) pole position ω_F (=33.8718 a.u.) on the ω axis (the free-ion graph is suppressed in the figure for the sake of visual clarity, as it lies on the outer part of, but quite close to, graph B). Thus, this offers a useful insight, where two different properties of the atomic system, e.g., the transition energy and the polarizability, have been correlated, and the plasma polarization redshift of the transition energy in the high-density regime is interpreted as a consequence of the density-induced enhancement in the system's polarizability or linear field response. The polarizability expresses a quantitative measure of the distortion of the bound-electron cloud under the action of an external field; high density-induced screening effects loosen up the orbitals that are now more diffuse and are likely to favor a larger polarizability, i.e., an increased deformability of the bound-electron cloud.

In Fig. 2, the amount of redshift of the $1s^2\,{}^1S \rightarrow 1s2p\,{}^1P$ line energy of the Ne^{8+} atomic ion is shown as a function of plasma electron density n_e. Quite substantial shifts, from $\sim$5 eV at $n_e \sim 1.6 \times 10^{24}$ cm^{-3} up to $\sim$55 eV at $n_e \sim 1.3 \times 10^{25}$ cm^{-3}, are obtained. A magnitude of the shift $\sim$19.6 eV at $n_e \sim 6.0 \times 10^{24}$ cm^{-3} as obtained in the present calculation may be compared against the shift $\sim$17.4 eV at $n_e \sim 6.0 \times 10^{24}$ cm^{-3} and the electron temperature $T_e \sim 500$ eV computed in Ref. [44], employing both the temperature-dependent self-consistent field ion-sphere model and the quantum-mechanical impact methods. In addition, the calculation of $\alpha_d(\omega)$ enables us to obtain the absorption oscillator strength (in the length form expressed in a.u.) $f_{\rm abs}(m \rightarrow n) = (2/3)\omega_{mn}[\langle m|\mathbf{r}|n\rangle]^2$, which is derivable from $\alpha_d(\omega)$ via the standard expression $\alpha_d(\omega) = \Sigma_{n \neq m} f_{\rm abs}(m \rightarrow n)/(\omega_{mn}^2 - \omega^2)$. In Fig. 3, the variation of $f_{\rm abs}(1s^2\,{}^1S \rightarrow 1s2p\,{}^1P)$ for the Ne^{8+} ion with the plasma electron density n_e is presented. It is observed that $f_{\rm abs}$ decreases monotonically with n_e, and the free-ion (i.e., $n_e = 0$) value of 0.7211 (that agrees well with the theoretical value

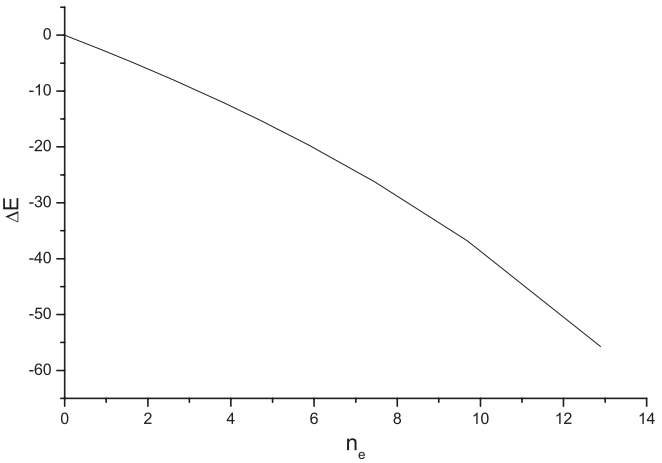

FIG. 2. The redshift ΔE (in eV) of the $1s^2\,{}^1S \rightarrow 1s2p\,{}^1P$ transition energy of a Ne^{8+} atomic ion, as a function of plasma electron density n_e (in 10^{24} cm^{-3}).

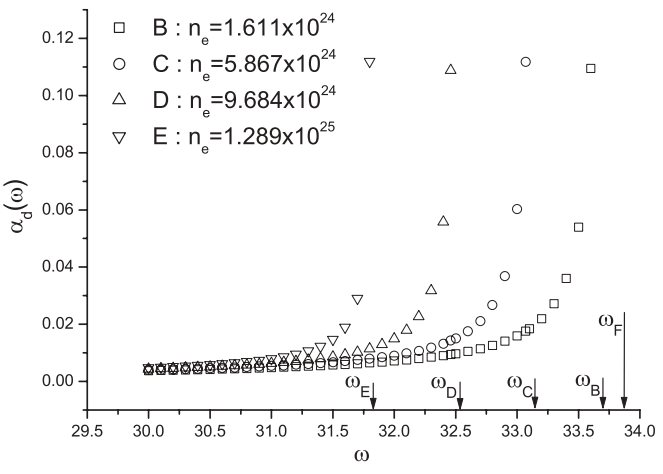

FIG. 1. Variation of the frequency-dependent dipole polarizability $\alpha_d(\omega)$ (in a.u.) of a Ne^{8+} atomic ion in ground state $1s^2\,{}^1S$ with the incident field frequency ω (in a.u.) at different plasma electron densities n_e (in cm^{-3}).

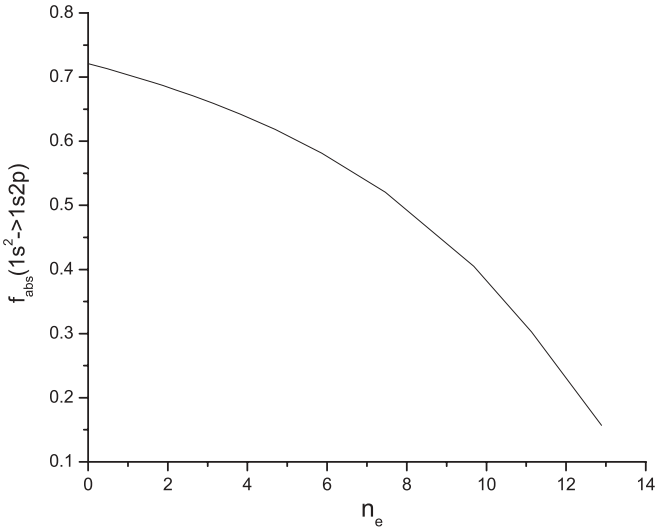

FIG. 3. Absorption oscillator strength $f_{\rm abs}$ $(1s^2\,{}^1S \rightarrow 1s2p\,{}^1P)$ (dimensionless) as a function of plasma electron density n_e (in 10^{24} cm^{-3}) for a Ne^{8+} atomic ion.

0.7226 of Ref. [45]) suffers a reduction of ∼80% at a density $n_e \sim 1.3 \times 10^{25}$ cm^{-3}.

IV. CONCLUSION

We have reported here the results of our investigation on the effects of plasma electron density on frequency-dependent polarizability of a heliumlike atomic ion based on a uniform-density ion-sphere model incorporated within a time-dependent coupled Hartree-Fock scheme. Our study indicates a connection between atomic polarizability and plasma density-induced line shift, and demonstrates that the redshift of the atomic transition energy in the high-density regime emerges naturally as a consequence of density-induced enhancement of atomic dynamic polarizability. The density-dependent data for dynamic polarizability, transition energy shift, and absorption oscillator strength presented in this calculation are mostly new, and possible improvements in these atomic data might be sought within the framework of a more sophisticated self-consistent field ion-sphere model [44]. The temperature-independent uniform-density ion-sphere model employed in this study provides approximate results for the plasma density effects on atomic structures for a mildly strongly coupled plasma with a relatively high electron temperature that makes the number density of plasma electrons within the ion sphere spatially independent. Therefore, the results presented here may be considered as the limiting values at high temperatures. On the other hand, in the self-consistent field ion-sphere model, the spatial distribution of the plasma electrons within the ion sphere is temperature dependent. With the inclusion of temperature, the present data are likely to suffer quantitative changes as the temperature is gradually reduced (it may be noted that, in Fig. 2 of Ref. [44], the plasma polarization shift is observed to grow in magnitude at reduced temperatures); hence, it is logical to anticipate that the conclusions made in the earlier parts of this paper on the basis of our present results are valid in a qualitative way. Additionally, it must be remembered that, in reality, an atomic line shift in a plasma can be a complex, cumulative effect owing to a number of processes (arising from temperature, static, and dynamic fields, etc.), while in the present paper we have concentrated only on the shift owing to an isolated process, e.g., the plasma polarization shift that owes its origin to plasma density-induced static screening effects around the radiating atomic ion. Still, on the basis of the present calculation, it seems that whatever mechanism or "perturbation" (single or multiple) is responsible for the cumulative shift, if all such perturbations are properly represented in H_0, then the theoretically estimated frequency-dependent polarizability of the lower state involved in the atomic transition in the plasma-embedded atom should also reflect the cumulative shift. Thus, the present linear response-based technique might effectively be employed to determine and provide an independent verification of atomic line shifts (as well as to estimate oscillator strengths and transition rates also) within dense plasmas, in order to corroborate the observations and conclusions based on traditional theoretical as well as experimental investigations. Also, more elaborate studies on several two-electron atomic ions should be useful for studying and formulating the expressions for the isoelectronic variation (e.g., the Z dependence) of atomic properties in the presence of the plasma electron density. Such variations must be different from those already established for free ions and would be considered in our future program.

ACKNOWLEDGMENTS

J.B. is grateful to the BESU, Shibpur for support. The authors thank the anonymous referees for valuable comments.

[1] D. Salzmann, *Atomic Physics in Hot Plasmas* (Oxford University Press, New York, 1998), Chap. 3 and relevant references therein.
[2] S. Skupsky, Phys. Rev. A **21**, 1316 (1980).
[3] D. Ray and P. K. Mukherjee, Eur. Phys. J. D **2**, 89 (1998).
[4] D. Ray and P. K. Mukherjee, J. Phys. B **31**, 3479 (1998).
[5] D. Ray, Phys. Rev. E **62**, 4126 (2000).
[6] D. Ray, J. Phys. B **33**, L21 (2000).
[7] D. Ray, Phys. Rev. E **63**, 027401 (2001).
[8] L. B. Zhao and Y. K. Ho, Phys. Plasmas **11**, 1695 (2004).
[9] S. Sahoo and Y. K. Ho, Phys. Plasmas **13**, 063301 (2006).
[10] S. Kar and Y. K. Ho, Phys. Rev. E **70**, 066411 (2004).
[11] S. Kar and Y. K. Ho, Phys. Rev. A **71**, 052503 (2005).
[12] S. Kar and Y. K. Ho, Phys. Rev. A **72**, 010703(R) (2005).
[13] S. Kar and Y. K. Ho, Chem. Phys. Lett. **424**, 403 (2006).
[14] A. C. H. Yu and Y. K. Ho, Phys. Plasmas **12**, 043302 (2005).
[15] Y. Y. Qi, J. G. Wang, and R. K. Janev, Phys. Rev. A **80**, 032502 (2009).
[16] D. Bielinska-Waz, J. Karwowski, B. Saha, and P. K. Mukherjee, Phys. Rev. E **69**, 016404 (2004).
[17] H. Okutsu, T. Sako, K. Yamanouchi, and G. H. F. Diercksen, J. Phys. B **38**, 917 (2005).
[18] B. Saha and S. Fritzsche, Phys. Rev. E **73**, 036405 (2006).
[19] B. Saha and S. Fritzsche, J. Phys. B **40**, 259 (2007).
[20] P. K. Mukherjee, S. Fritzsche, and B. Fricke, Phys. Lett. A **360**, 287 (2006).
[21] S. Kar and Y. K. Ho, Phys. Lett. A **368**, 476 (2007).
[22] L. Liu, J. G. Wang, and R. K. Janev, Phys. Rev. A **77**, 032709 (2008).
[23] Y. Y. Qi, J. G. Wang, and R. K. Janev, Phys. Rev. A **80**, 063404 (2009).
[24] S. Paul and Y. K. Ho, Phys. Plasmas **15**, 073301 (2008).
[25] S. Paul and Y. K. Ho, Phys. Rev. A **78**, 042711 (2008).
[26] S. Paul and Y. K. Ho, Phys. Rev. A **79**, 032714 (2009).
[27] S. Paul and Y. K. Ho, J. Phys. B **43**, 065701 (2010).
[28] J. C. Weisheit, Adv. At. Mol. Phys. **25**, 101 (1988).
[29] M. S. Murillo and J. C. Weisheit, Phys. Rep. **302**, 1 (1998).
[30] D. Salzmann and H. Szichman, Phys. Rev. A **35**, 807 (1987).
[31] Y. D. Jung, Eur. Phys. J. D **7**, 249 (1999), and relevant references therein.
[32] C. C. J. Roothaan, Rev. Mod. Phys. **23**, 69 (1951).

[33] E. Clementi and C. Roetti, At. Data Nucl. Data Tables **14**, 177 (1974), and relevant references therein.
[34] H. Friedrich, *Theoretical Atomic Physics* (Springer, Berlin, 1991), Sec. 3.4.3.
[35] M. Karplus and H. J. Kolker, J. Chem. Phys. **38**, 1263 (1963).
[36] M. Karplus and H. J. Kolker, J. Chem. Phys. **39**, 1493 (1963); **39**, 2011 (1963); **39**, 2997 (1963).
[37] B. Kundu, D. Ray, and P. K. Mukherjee, Phys. Rev. A **34**, 62 (1986).
[38] P. K. Mukherjee, K. Ohtsuki, and K. Ohno, Theor. Chim. Acta **74**, 431 (1988).
[39] J. Heinrichs, Phys. Rev. **172**, 1315 (1968).
[40] P. W. Langhoff, S. T. Epstein, and M. Karplus, Rev. Mod. Phys. **44**, 602 (1972).
[41] P. O. Löwdin and P. K. Mukherjee, Chem. Phys. Lett. **14**, 1 (1972).
[42] L. A. Vainshtein and U. I. Safronova, At. Data Nucl. Data Tables **21**, 49 (1978).
[43] J. F. Thornbury and A. Hibbert, J. Phys. B **20**, 6447 (1987).
[44] M. Koenig, P. Malnoult and H. Nguyen, Phys. Rev. A **38**, 2089 (1988).
[45] N. M. Cann and A. J. Thakkar, Phys. Rev. A **46**, 5397 (1992).